

Observations on dA scattering at forward rapidities

V. Guzey^a, M. Strikman^b, and W. Vogelsang^c

^a *Institut für Theoretische Physik II, Ruhr-Universität Bochum, D-44780 Bochum, Germany*

^b *Department of Physics, Pennsylvania State University, University Park, PA, U.S.A.*

^c *Physics Department and RIKEN-BNL Research Center,
Brookhaven National Laboratory, Upton, New York 11973, U.S.A.*

Abstract

We point out that the suppression in the ratio R_{dAu} recently observed by the BRAHMS collaboration in forward scattering is stronger than usually appreciated. This is related to the fact that at forward rapidities BRAHMS measures negatively charged hadrons and that R_{dAu} is defined from the ratio of dA and pp scattering cross sections. We also investigate the influence of standard shadowing on R_{dAu} , and the typical values of partonic momentum fractions relevant in forward scattering. We find that $x_{\text{Au}} \geq 0.02$ dominate in the cross section.

I Introduction

The BRAHMS collaboration has recently presented measurements of the ratio R_{dAu} of hadron production cross sections in dAu and pp collisions [1]. With increasing hadron rapidity, the data indicate a growing suppression of the ratio. Theoretical analyses of the data have focused on nuclear effects related to the gold nucleus, emphasizing variously the role of small x physics in the nuclear production [2], as well as of nuclear-enhanced power corrections in the dA cross section [3]. Other studies [4, 5] have addressed the question of whether leading-twist shadowing could be responsible for the observed suppression.

In the present paper we hope to add valuable information that will have an impact on the present and future attempts to interpret the BRAHMS data, and on plans for further measurements. We base our analysis on next-to-leading order (NLO) leading-twist perturbative-QCD (pQCD) calculations of inclusive hadron production. Such calculations have enjoyed considerable success in comparisons with data from pp collisions at RHIC at $\sqrt{s} = 200$ GeV. They yield good agreement with the PHENIX data [6] for $pp \rightarrow \pi^0 X$ at central rapidities, and with data from STAR [7] on $pp \rightarrow \pi^0 X$ at forward rapidities $\eta = 3.8$ and $\eta = 3.3$, the latter being essentially in the kinematic range explored by BRAHMS in their most forward measurements. It is appropriate to point out that there are sizable uncertainties in the NLO calculation, related to the choice of fragmentation functions and scales. However, we are confident that for the kinematics relevant for BRAHMS NLO pQCD does explain at least 50% of the cross section, as a conservative estimate, and hence is a viable tool for obtaining deeper insights into the production mechanism, at least for pp collisions.

The main point of our analysis can be stated very simply: the nuclear effect reported by BRAHMS actually appears to be substantially larger than appreciated in the studies [2, 3, 5]. This is related to the fact that in the very forward region, at rapidities $\eta = 2.2$ and $\eta = 3.2$, BRAHMS only measured *negatively charged* hadrons (h^-) and not the charge average $(h^+ + h^-)/2$ as at the more central rapidities. In the ratio R_{dA} the denominator refers to pp collisions, and negatively charged hadrons are expected to be produced more rarely in pp than in dA collisions, for which from isospin considerations it follows that at least π^+ and π^- should be produced in equal numbers. This immediately implies that the ratio of $\text{dAu} \rightarrow h^- X$ and $pp \rightarrow h^- X$ cross sections is “intrinsically enhanced”, by actually a factor of about 1.5, as we will show. The fact that BRAHMS nonetheless reports a suppression of the ratio is therefore truly remarkable and awaits further investigation.

We also revisit in our analysis the following questions:

- (i) what are the most relevant parton momentum fractions x for hadron production at BRAHMS, in particular at very forward rapidity $\eta = 3.2$ where the suppression of R_{dA} is largest? To what extent are truly small x , say, $x < 10^{-3}$ probed?
- (ii) how relevant is leading-twist nuclear shadowing for the explanation of the BRAHMS data?

These questions have already been addressed in some detail in [5]. Our analysis extends that study by providing results within a full NLO calculation. This will generally lead to more reliable results. In addition, the enhancement effect mentioned above has of course also direct implications for estimates for R_{dA} obtained when using leading-twist nuclear shadowing. Our calculations therefore provide an improved estimate as compared to the results of [5], where the enhancement was not taken into account. We furthermore explore more thoroughly the possible effects of leading-twist nuclear shadowing by making more extreme assumptions on the structure of screening at intermediate x , tolerated because of possible uncertainties in the connection between diffractive HERA data and gluon shadowing.

In sec. II we discuss the ranges of partonic momentum fractions mainly probed by the forward BRAHMS data. Section III addresses the leading-twist nuclear shadowing and its relevance in forward dA scattering. With the findings of sections II and III, we are in the position to discuss R_{dA} in the forward region in more detail. This is done in Section IV, where we emphasize our main point related to the normalization of R_{dA} by the $pp \rightarrow h^- X$ cross section. We summarize and conclude with section V.

II Kinematics and x ranges probed in forward scattering

We consider the reaction $H_1 H_2 \rightarrow h X$, where H_1, H_2 are initial hadrons and h is a hadron in the final state produced at high transverse momentum p_T . Since large p_T ensures large momentum transfer, the cross section for the process may be written in a factorized form,

$$\begin{aligned}
 d\sigma = & \sum_{a,b,c} \int_{x_2^{\text{min}}}^1 dx_2 \int_{x_1^{\text{min}}}^1 dx_1 \int_{z^{\text{min}}}^1 dz f_a^{H_1}(x_1, \mu) f_b^{H_2}(x_2, \mu) D_c^h(z, \mu) \\
 & \times d\hat{\sigma}_{ab}^c(x_1 P_{H_1}, x_2 P_{H_2}, P_h/z, \mu) ,
 \end{aligned} \tag{1}$$

where the sum is over all contributing partonic channels $a+b \rightarrow c+\dots$, with $d\hat{\sigma}_{ab}^c$ the associated short-distance cross section which may be evaluated in QCD perturbation theory:

$$d\hat{\sigma}_{ab}^c = d\hat{\sigma}_{ab}^{c,(0)} + \frac{\alpha_s}{\pi} d\hat{\sigma}_{ab}^{c,(1)} + \dots \tag{2}$$

The leading-order (LO) contributions $d\hat{\sigma}_{ab}^{c,(0)}$ are of order α_s^2 ; the next-to-leading order (NLO) corrections are known [8] and will be included in our analysis.

In Eq. (1), $f_i^H(x, \mu)$ denotes the distribution function at scale μ for a parton of type i in hadron H , carrying the fraction x of the hadron's light-cone momentum. Likewise, $D_c^h(z, \mu)$ describes the fragmentation of produced parton c into the observed hadron h , the latter taking momentum fraction z of the parton momentum. The scale μ in Eq. (1) stands generically for the involved renormalization and factorization scales. μ should be of the order of the hard scale in the process; in the following we choose $\mu = p_T$. The dependence on μ is actually quite large even at NLO [8]; however, in this work we are mainly interested in ratios of cross sections for which the μ dependence is fairly insignificant.

The lower limits of the integrations over momentum fractions in Eq. (1) may be derived in terms of $x_T = 2p_T/\sqrt{s}$ and the pseudorapidity η of the produced hadron. They are given by

$$\begin{aligned} x_2^{min} &= \frac{x_T e^{-\eta}}{2 - x_T e^{\eta}} , \\ x_1^{min} &= \frac{x_2 x_T e^{\eta}}{2x_2 - x_T e^{-\eta}} , \\ z^{min} &= \frac{x_T}{2} \left[\frac{e^{-\eta}}{x_2} + \frac{e^{\eta}}{x_1} \right] . \end{aligned} \quad (3)$$

From these equations it follows that at central rapidities $\eta \approx 0$ the momentum fractions x_1 and x_2 can become as small as roughly p_T/\sqrt{s} . In *forward* scattering, that is, at (large) positive η , the collisions become very asymmetric. In particular, x_2 may become fairly small, whereas x_1 tends to be large. For forward kinematics at BRAHMS one has, typically, $p_T \sim 1.5$ GeV and $\eta = 3.2$. This implies that x_2 may become as small as $\sim 3.5 \times 10^{-4}$. However, in practice it turns out that such small x_2 hardly ever contribute to the cross section: if x_2 is so small, the hadron with transverse momentum p_T can only be produced if both x_1 and z are unity, where however the parton distributions $f_a^{H_1}(x_1, \mu)$ and the fragmentation functions $D_c^h(z, \mu)$ vanish. This is an immediate consequence of kinematics, as demonstrated by Eqs. (3). One can show that if the parton density $f_a^{H_1}(x_1, \mu)$ behaves at large x_1 as $(1 - x_1)^{a_f}$ and $D_c^h(z, \mu)$ as $(1 - z)^{a_D}$ (with some powers $a_f, a_D \gg 1$), the x_2 -integrand in Eq. (1) vanishes in the vicinity of x_2^{min} as $(x_2 - x_2^{min})^{a_f + a_D + 1}$. Therefore, contributions from very small x_2 are highly suppressed.

The question, then, remains of how small x_2 really is on average for forward kinematics at RHIC. This is of course relevant for judging various explanations for the suppression of R_{dA} seen by BRAHMS, in particular those relating to saturation effects in the nucleus wave function [2]. Figure 1 shows the distribution of the cross section for $pp \rightarrow \pi^0 X$ at $\sqrt{s} = 200$ GeV, $p_T = 1.5$ GeV, $\eta = 3.2$, in bins of $\log_{10}(x_2)$. The overall normalization is unimportant of

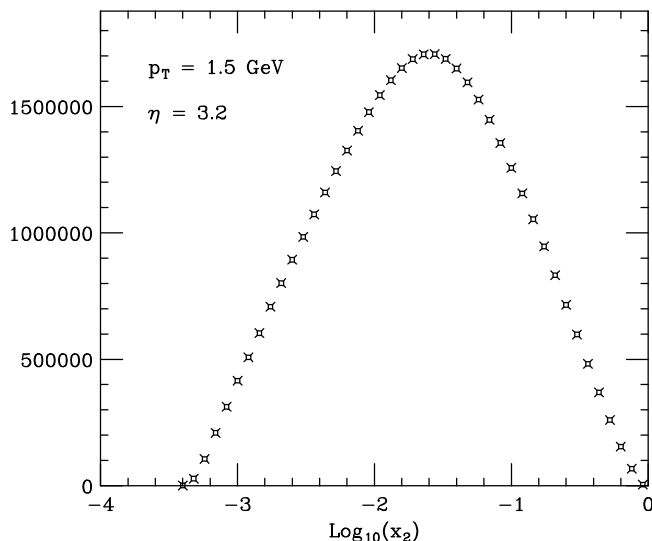


Figure 1: Distribution in $\log_{10}(x_2)$ of the NLO invariant cross section $Ed^3\sigma/dp^3$ at $\sqrt{s} = 200$ GeV, $p_T = 1.5$ GeV and $\eta = 3.2$.

course; for definiteness we note that the sum of all entries shown in the plot yields the full NLO invariant cross section $Ed^3\sigma/dp^3$ in pb/GeV^2 . For the calculation we have chosen the CTEQ6M [9] parton distribution functions and the fragmentation functions of Ref. [10]. One can see that the distribution peaks at $x_2 > 0.01$. There are several ways to estimate an average $\langle x_2 \rangle$ of the distribution. For example, one may define $\langle x_2 \rangle$ in the standard way from evaluating the integral in Eq. (1) with an extra factor x_2 in the integrand, divided by the integral itself:

$$\langle x_2 \rangle \equiv \frac{\int_{x_2^{\min}}^1 dx_2 x_2 f_b^{H_2}(x_2, \mu) \dots}{\int_{x_2^{\min}}^1 dx_2 f_b^{H_2}(x_2, \mu) \dots}, \quad (4)$$

where the ellipses denote the remaining factors in Eq. (1). Alternatively, one may simply determine $\langle x_2 \rangle$ as the median of the distribution, demanding that the area under the distribution in Fig. 1 to the left of $\langle x_2 \rangle$ equals that to the right. Either way, one finds an average $\langle x_2 \rangle > 0.01$, typically $0.03 - 0.05$ at this p_T and η .

The precise shape of the distribution and the value of $\langle x_2 \rangle$ depend somewhat on the parton distributions (and, less so, on the fragmentation functions) chosen. We remind the reader that the distribution shown in Fig. 1 is at $p_T = 1.5$ GeV and that we have chosen the factorization and renormalization scales to be $\mu = p_T$. This means that we are using a fairly low scale in the parton densities. At this scale, the CTEQ6 densities, in particular the gluon, are still relatively flat towards small x . In order to estimate to what extent this influences the distribution, we have calculated it for the GRV [11] parton distributions, which are steeper at this scale. The corresponding histogram in $\log_{10}(x_2)$ is shown in Fig. 2. One can see that as expected it peaks somewhat more to the left; nevertheless there is not much quantitative change in the average

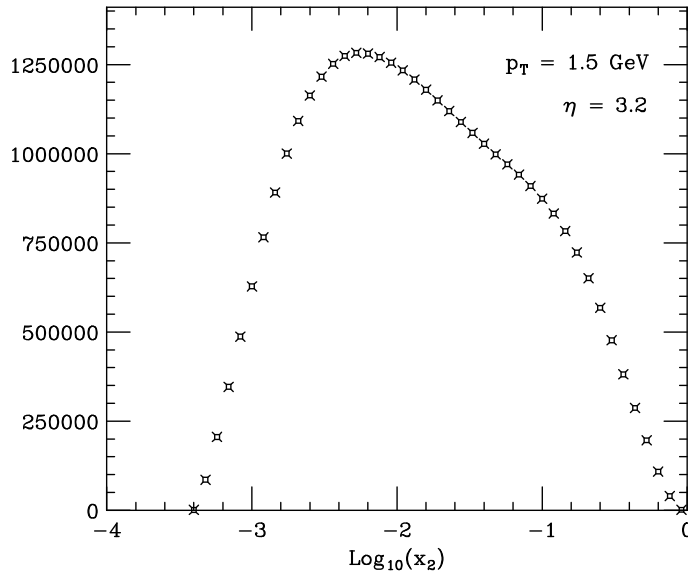


Figure 2: Same as Fig. 1 but for the GRV [11] parton distributions.

x_2 . The full invariant cross section is about 15% smaller than for the CTEQ6 set. We have mentioned in the introduction that there are data from STAR for the cross section for $pp \rightarrow \pi^0 X$ in roughly this kinematic range [7] which are in very good agreement with the NLO calculation used in Fig. 1. This supports the view that the distributions shown in Figs. 1 and 2 are realistic.

Figure 3 shows the $\log_{10}(x_2)$ distribution at $p_T = 5$ GeV. At this p_T , one is closer to the boundary of phase space given by the condition $x_T \cosh(\eta) = 1$, where all momentum fractions x_1, x_2, z are forced to 1. The distribution in x_2 is therefore more “squeezed” and shifted to the right. The effect is countered to some extent by evolution since at scale $\mu = 5$ GeV the parton distributions are steeper than at $\mu = 1.5$ GeV.

Finally, in Figure 4 we present results for the averages of x_1 , x_2 , and z , as functions of pion transverse momentum and rapidity at $\sqrt{s} = 200$ GeV. Here we have defined $\langle x_2 \rangle$ as in Eq. (4), with analogous definitions for $\langle x_1 \rangle$ and $\langle z \rangle$. The upper row shows results for fixed p_T in forward scattering. Besides $\eta = 3.2$ as relevant for BRAHMS, we have also extended the results to $\eta = 4.2$ which may be useful for future experimental studies. It becomes evident that $\langle x_1 \rangle$ and $\langle z \rangle$ are very large in forward scattering, as expected. $\langle z \rangle$ is particularly large because, on account of Eq. (1), the single fragmentation function has to compete with two parton densities, each function being strongly suppressed at large momentum fraction. As we have already seen in the histograms, Figs. 1–3, $\langle x_2 \rangle$ is much smaller. As p_T increases and the boundary of phase space is approached, all momentum fractions become larger and eventually converge to unity. We also note an unexpected upturn of $\langle x_2 \rangle$ toward smaller p_T . We have

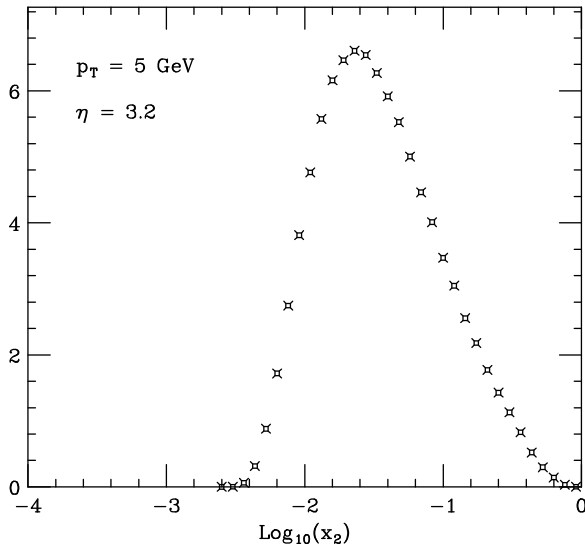


Figure 3: Same as Fig. 1, but for $p_T = 5$ GeV.

not been able to identify this effect as resulting from any straightforward origin. The precise small- x behavior of the parton distributions at the rather low scales involved here plays a role (however, the effect also occurs for the steeper GRV distributions). The structure of the cross section formula in Eq. (1) itself is also partly responsible. In the lower part of Fig. 4 we show the averages as functions of rapidity for two fixed values of p_T . At $\eta = 0$ one obviously starts from $\langle x_1 \rangle = \langle x_2 \rangle$; with increasing η the two momentum fractions become very different. Toward $\eta = \cosh^{-1}(1/x_T)$ they again both tend to unity; for $\langle x_2 \rangle$ this happens rather late.

III Influence of leading-twist nuclear shadowing

In dA collisions, nuclear effects will alter the distribution in x_2 as well as the full cross section. Shadowing effects at small- x_2 , $x_2 < 0.05 - 0.1$, will lower the cross section and will lead to yet higher average x_2 being probed. There will also be enhancements at larger x_2 , $0.05 - 0.1 < x_2 < 0.2$, associated with yet another coherent nuclear effect, antishadowing. This will be followed by the suppression related to the EMC effect for $0.2 < x_2 < 0.8$, and by the subsequent enhancement explained by the Fermi motion for $x_2 > 0.8$.

Since in the BRAHMS kinematics the average x_2 is near 0.01, the principal nuclear effect is shadowing. We investigate its role in the interpretation of the BRAHMS data by considering leading-twist shadowing, using the parameterization of nuclear parton distribution functions (nPDFs) derived in [12, 13, 14]. Unlike most other sets of nPDFs [4, 15], these functions have a rather rapid and strong onset of shadowing toward small- x , so they may serve as a good tool

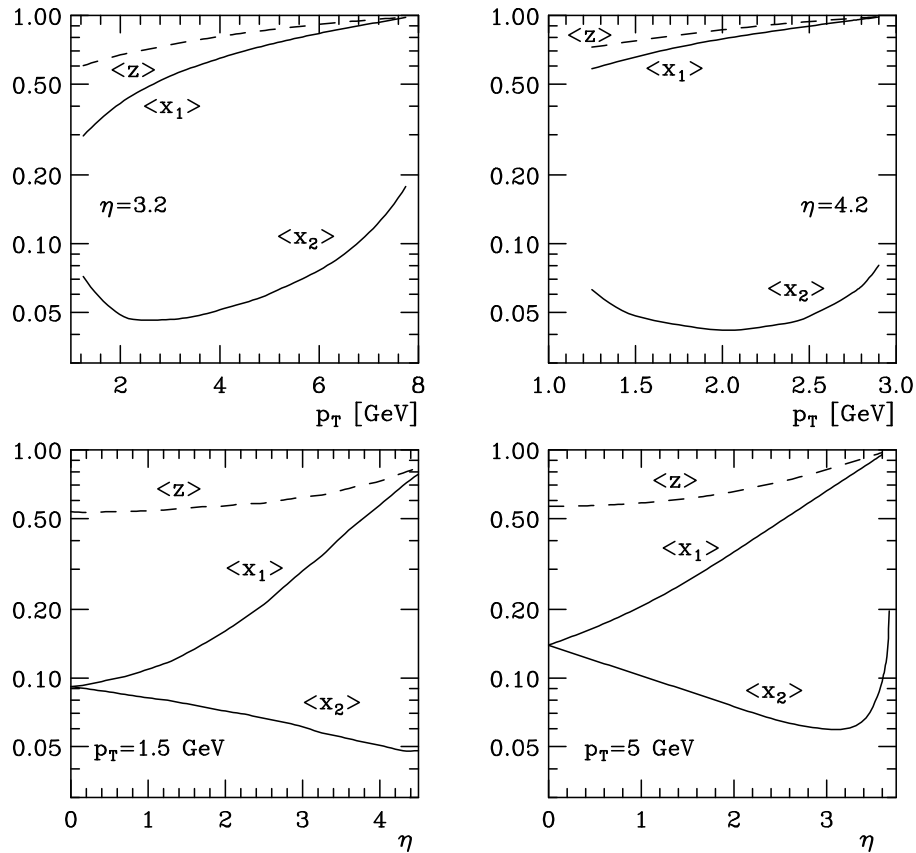


Figure 4: Averages of x_1 , x_2 , and z in $pp \rightarrow \pi^0 X$ at RHIC, defined as in Eq. (4), as functions of pion transverse momentum at forward rapidities (upper row), and of pion rapidity for fixed p_T (lower row).

for studying the “maximally possible” effects of leading-twist nuclear shadowing in forward dA scattering. The recent study [5] has also employed the nPDFs of [12, 13, 14], albeit only in the framework of a lowest order (LO) calculation.

We note that we will neglect any nuclear effects in the deuteron, for which we just use $d = (p+n)/2$. As follows from our analysis of the average x_1 , the deuteron parton distributions are sampled at values of x_1 in the domain of the EMC effect. Therefore, the approximation $d = (p+n)/2$ is valid to a few per cent accuracy, as can be estimated as follows. The CTEQ fits use the neutron structure function extracted from the deuteron data within the framework of the convolution approximation (Fermi motion). The convolution model gives for the structure function ratio $R = 2F_2^d/(F_2^p + F_2^n)$ the values of 0.99 for $x \sim 0.5$ and of 1.03–1.05 for $x \sim 0.7$. As a result, our $d = (p+n)/2$ approximation overestimates the true deuteron parton distributions by about $\sim 1\%$ at $x \sim 0.5$ and underestimates them by a few percent at $x \sim 0.7$. Since large x_1 are important in our calculations, proper account of this would make the effect we will discuss

in the next section even slightly bigger. Note that for heavier nuclei the convolution model contradicts the EMC effect. However here we are using it to “restore” the deuteron structure function within the procedure used to extract the neutron structure function; see [16] for an extensive discussion of nuclear effects in the deuteron parton densities.

Let us now briefly describe the approach of [12, 13, 14] for deriving nPDFs. Leading-twist nuclear shadowing is obtained using Gribov’s theorem [17] relating nuclear shadowing to diffraction, Collins’s QCD factorization theorem for hard diffraction in DIS [18], and the QCD analysis of hard diffraction measured at HERA in terms of diffractive parton distribution functions of the proton. Operationally, the nPDFs are first derived at the initial scale $Q_0=2$ GeV and for $10^{-5} \leq x \leq 1$. Standard (NLO) DGLAP evolution is then used to obtain the nPDFs for $Q^2 > Q_0^2$.

Analyses of DIS by both H1 [19] and ZEUS [20] demonstrate that diffraction constitutes $\approx 10\%$ of the total cross section in the quark-dominated channel and as much as $\approx 30\%$ in the gluon channel. As a result, it is found in [12, 13, 14] that the effect of nuclear shadowing in nPDFs is large and, even more strikingly, much stronger in the gluon nPDF at small x than in the quark nPDFs.

Conservation of the baryon number and the momentum sum rule then require that the depletion of nPDFs at small values of x , $x < 0.01$, be accompanied by a certain enhancement at $0.05 < x < 0.2$. The transition from shadowing to enhancement, and the enhancement itself, are not described by the Gribov theorem and, hence, can be only modeled. Using the available fixed-target nuclear DIS data [21] as a guide, the “standard” scenario of [12, 13, 14] assumes that the transition from nuclear shadowing to the enhancement takes place at $x = 0.1$ for quark nPDFs, and at $x = 0.03$ for the gluon nPDF. In the following, we will refer to this set of nPDFs as “shadowing 1”.

Figure 5 shows the distribution of the NLO cross section for $dAu \rightarrow \pi^0 X$ in $\log_{10}(x_2)$, using shadowing 1. For comparison, we also display the previous result for $pp \rightarrow \pi^0 X$ of Fig. 1 (solid line). A clear shift in the distribution to larger x_2 is visible. At small x_2 , there are significant shadowing effects, while at large x_2 there is a small contribution from antishadowing. It is evident from comparison of the areas underneath the distributions that the net effect on the dAu cross section will be a decrease. However, one can anticipate that the decrease will be rather moderate: while nuclear shadowing does deplete the dA cross section compared to the pp cross section, the probed values of x_2 are clearly not small enough to deliver a significant nuclear shadowing effect.

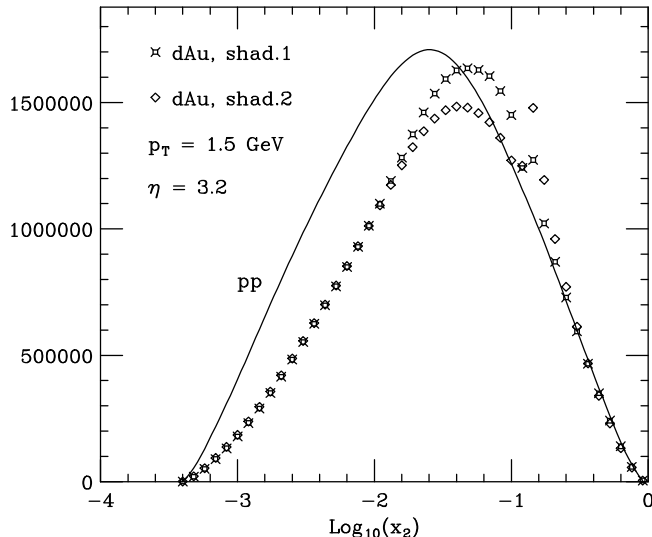


Figure 5: Same as Fig. 1, but also showing the result for dAu scattering using the shadowing of Refs. [12, 13, 14], and a more extreme ansatz for shadowing (see text). The “spikes” in the distributions at $\log_{10}(x_2) \approx -0.8$ are artifacts of the implementation of antishadowing in the nPDFs of [12, 13, 14]. For better comparison we have displayed the result of Fig. 1 by a solid line.

The kinematics for forward scattering at BRAHMS mostly corresponds to values of x_2 in the transition region between shadowing and antishadowing, where the predictions for nPDFs are rather uncertain. Therefore, in addition to the standard scenario (“shadowing 1”) of nuclear shadowing, we have also explored an option for which nuclear shadowing in the gluon channel is increased by extending it up to $x = 0.1$, similarly to the shadowing in the quark densities. We refer to the resulting set of nPDFs as “shadowing 2”. The corresponding $\log_{10}(x_2)$ distribution of the cross section for $dAu \rightarrow \pi^0 X$ is also displayed in fig. 5. Compared to shadowing 1, there is only a small modification of the distribution, which will lead to a very slight further suppression of the dA cross section. It is worth emphasizing that one can hardly increase the amount of gluon shadowing at $x \sim 10^{-3}$ since here there are constraints from J/ψ data [22]. The model of [12, 13, 14] gives a reasonable description of the observed suppression by a factor ~ 2 , which would be spoiled by a much stronger gluon shadowing. At the same time, as soon as the amount of gluon shadowing at $x \sim 10^{-3}$ is fixed, the gradual decrease of shadowing with increasing x is automatic as a consequence of the decrease of the coherence length $\propto 1/m_N x$ and of a smaller probability for diffraction. Therefore, we conclude that the standard effect of leading twist nuclear shadowing will at best be able to explain only a small fraction of the dramatic suppression of the spectra of charged hadrons at forward rapidities observed by BRAHMS. This statement is in line with the LO result in the revised version of [5].

Figure 5 shows the corresponding results for $p_T = 5$ GeV. Here, larger x_2 are probed, and

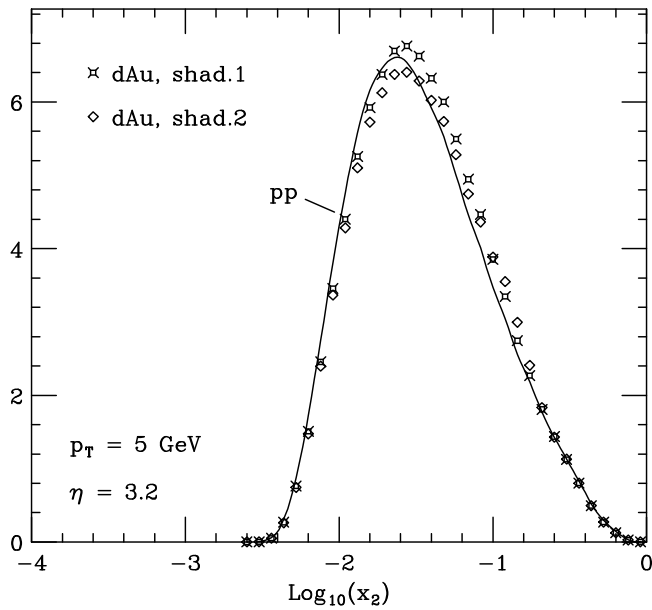


Figure 6: Same as Fig. 5, but at $p_T = 5$ GeV.

only slight antishadowing effects appear.

So far we have only considered π^0 production as an example. This is however not really appropriate for a comparison with the BRAHMS data which, at forward rapidities, are for negatively charged hadrons h^- . As we will now show, for the case of h^- , even in presence of the shadowing effects just discussed, the leading-twist NLO calculation predicts an *enhancement*, rather than a suppression, of R_{dA} .

IV Isospin considerations for the ratio of dA and pp cross sections

We now consider the ratio R_{dA} of single-inclusive hadron cross sections in dA and pp scattering. The BRAHMS experiment has presented data [1] for R_{dA} as a function of hadron transverse momentum p_T , in four different bins of hadron pseudorapidity η , with central values $\eta = 0, 1, 2.2, 3.2$. BRAHMS sees a significant suppression of the ratio with increasing η .

While BRAHMS measures inclusive charged hadrons, $(h^+ + h^-)/2$, at central rapidities ($\eta = 0$ and 1), their R_{dA} data at forward rapidities refer only to *negatively* charged hadrons h^- . This has profound consequences. To see this, let us assume for the moment that pions dominate the spectrum of observed high- p_T hadrons. Negatively charged pions are produced more rarely than positively charged ones in pp collisions, due to the up-quark dominance in the proton. An

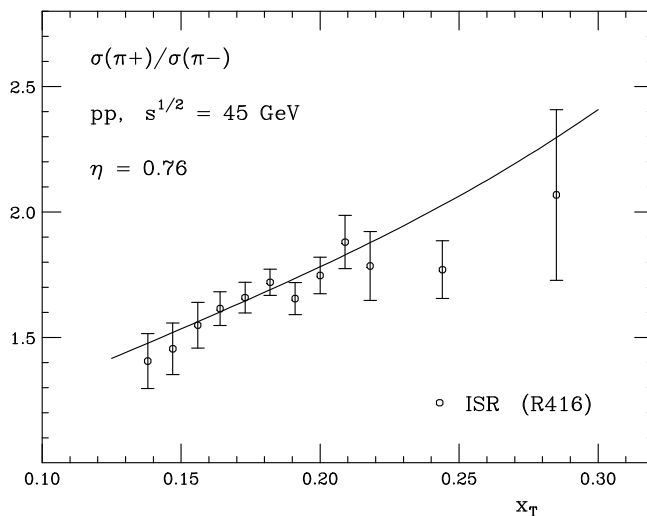


Figure 7: Ratio of $pp \rightarrow \pi^+ X$ and $pp \rightarrow \pi^- X$ cross sections at $\sqrt{s} = 45$ GeV and scattering angle 50° (corresponding to pseudorapidity $\eta = 0.76$), as a function of $x_T \equiv 2p_T/\sqrt{s}$. The data points are from measurements at the ISR [23]. The curve shows the result of the NLO calculation, using the fragmentation functions of [24].

example for this is shown in Fig. 7, where we display data for the π^+/π^- ratio from the ISR [23] at $\sqrt{s} = 45$ GeV. We also show the result of the NLO calculation, using the fragmentation functions of Ref. [24], which provides separate sets for negatively and positively charged pions. [We note that there are also π^+/π^- data at $\sqrt{s} = 62$ GeV [25] which lie lower and are in less impressive agreement with NLO pQCD.] As Fig. 7 shows, there is clear excess of positive pions over negative ones. In contrast, isospin considerations imply that π^+ and π^- are produced practically equally in dAu collisions. Therefore, one expects R_{dA} for negatively charged pions to be intrinsically enhanced, if it is normalized by the pp cross section and not, for example, by the dp one.

To go into a little more quantitative detail, we recall that at forward rapidities the partonic collisions are very asymmetric. Large contributions to the scattering come from situations in which a large- x_1 valence quark in the “projectile” (i.e., in the deuteron, or in one of the protons) hits a small- x_2 gluon in the “target” (i.e., in the gold nucleus or in the other proton). The underlying (LO) subprocess is then the quark-gluon Compton process $qg \rightarrow qg$. For negatively charged pions one then expects that down quarks play a particularly important role in the Compton process, since both the “projectile” and the produced π^- have a d valence quark. To a good approximation (see the previous section), the deuteron’s d valence density is given by

$$d_{val}^{deuteron} = \frac{1}{2} (d_{val}^p + d_{val}^n) = \frac{1}{2} (d_{val}^p + u_{val}^p), \quad (5)$$

where we have used isospin invariance to relate the valence- d distribution in the neutron to the

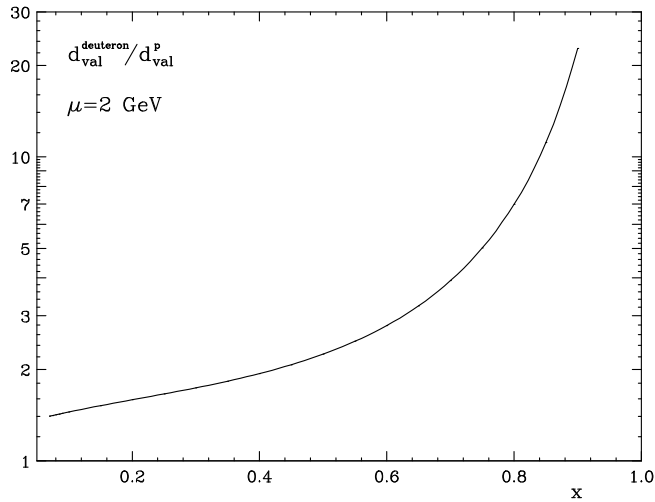


Figure 8: Ratio $d_{val}^{deuteron}(x)/d_{val}^p(x)$ as a function of x at the scale $\mu = 2$ GeV, as given by the CTEQ6M set. The deuteron's d -valence distribution has been estimated according to Eq. (5).

valence- u in the proton. Due to the up-quark excess in the proton, the distribution in Eq. (5) becomes much larger than the proton's d -valence distribution at high x , as shown in Fig. 8, resulting in an enhancement in R_{dA} . Of course, other scattering channels will contribute as well and dilute this valence effect. In addition, BRAHMS does not measure only pions, but inclusive charged hadrons, $h^\pm = \pi^\pm + K^\pm + \overset{(-)}{p} + \dots$. Nevertheless, when changing to charged-hadron fragmentation functions as given by [24], we find that the difference in deuteron and proton valence densities continues to play an important role in the forward production of negatively charged hadrons. This is demonstrated by Fig. 9. The solid lines show the ratio R_{dA} at $\eta = 0$ and 1 for *summed* charged hadrons $(h^+ + h^-)/2$, and at $\eta = 2.2$ and 3.2 for *negatively charged* hadrons, exactly corresponding to the BRAHMS conditions. We have used the “shadowing 1” set described in the previous section. As shown in sec. II, when going from $\eta = 0$ to $\eta = 1$, the average x_2 probed slightly decreases, and shadowing effects start to become visible at the smaller p_T . At $\eta = 2.2$ and $\eta = 3.2$ the x_2 become yet smaller, but since now negatively charged hadrons are measured, the valence effect discussed above outweighs any stronger shadowing, and in fact the ratio R_{dA} strongly increases with p_T because larger and larger x_1 become relevant. For comparison we also show in Fig. 9 the results at $\eta = 2.2$ and $\eta = 3.2$ for *summed* charged hadrons (dashed lines). For these, the effective valence densities in the proton and deuteron are the same, and the enhancement seen for negative hadrons disappears. Shadowing effects of up to 15% are visible then, as expected from Fig. 5, and as also found in Ref. [5] where only summed charged hadrons were considered. It is remarkable that for the highest $p_T \sim 3$ GeV at $\eta = 3.2$ the curve for h^- is enhanced by about a factor 1.5 with respect to the one for summed charges.

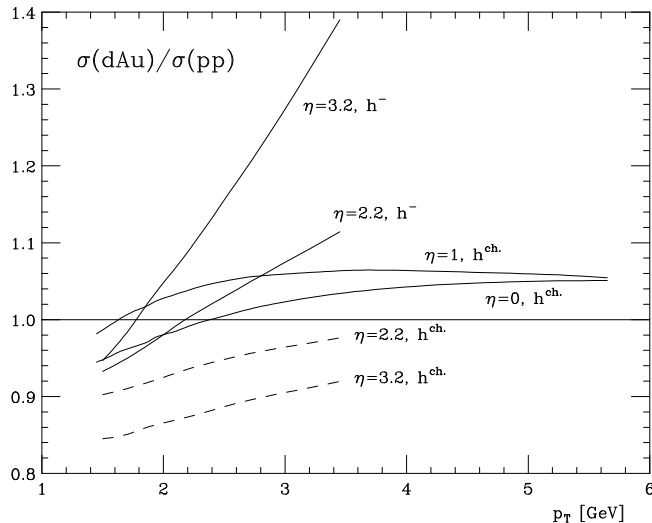


Figure 9: Ratio R_{dA} of cross sections for $\text{dAu} \rightarrow hX$ and $pp \rightarrow hX$ as a function of transverse momentum at various rapidities relevant to the BRAHMS experiment. As in experiment, we have considered production of *summed* charged hadrons, $h^{\text{ch}} \equiv (h^+ + h^-)/2$ for $\eta = 0, 1$ and *negatively* charged hadrons h^- for $\eta = 2.2$ and 3.2 . For comparison, the dashed lines show the result for summed charged hadrons at $\eta = 2.2$ and 3.2 . We have used the “shadowing 1” nPDFs for the gold nucleus. The fragmentation functions are from [24]; we have found that for the case of summed charged hadrons using the set of [10] does not alter our results by more than a few per cent.

Our analysis so far has been entirely based on a NLO pQCD leading-twist calculation and the use of fragmentation functions extracted from e^+e^- annihilation data. We expect that even if nonperturbative phenomena are important in the kinematic regime explored by BRAHMS, the enhancement in R_{dA} resulting due the different “projectiles” in the numerator and denominator will persist. Here, our reasoning is as follows: ISR data (see [26] and references therein) on π^\pm production at $p_T \sim 1$ GeV and large Feynman- $x_F \sim 0.4$ were found to be consistent with $d\sigma^{pp \rightarrow \pi^+}/dx_F \propto u(x_F)$, $d\sigma^{pp \rightarrow \pi^-}/dx_F \propto d(x_F)$, where u and d are typical densities for up and down valence quarks. Such spectra in x_F are much harder than the ones pQCD would give, indicating the presence of a nonperturbative production mechanism. Nonetheless, the ratio of π^+ to π^- cross sections is of a similar magnitude as the one in the perturbative regime shown in Fig. 7. Adding the fact that the yields of π^+, π^-, π^0 in dA scattering should be equal because of isospin, irrespective of the production mechanism, we are led to the conclusion that R_{dA} for negatively charged hadrons should be enhanced even if nonperturbative effects dominate. Note here that nonperturbative effects in the fragmentation region are known to be consistent with the Feynman scaling. Hence if nonperturbative effects are important they should lead to about the same π^+/π^- ratio in pp scattering for the same x_F at ISR and at RHIC.

We finally note that a potential caveat to our main finding in Fig. 9 comes from a further set

of BRAHMS data. While we have mentioned that BRAHMS measures all hadrons and not just pions, we have generally assumed that pions dominate the observed hadron spectrum. However, preliminary data from BRAHMS [27] show that the cross section for $dAu \rightarrow h^+ X$ becomes significantly larger than that for $dAu \rightarrow h^- X$ at $p_T > 1$ GeV. At $p_T = 3$ GeV, they observe about three times as many h^+ as h^- . As we have pointed out before, isospin excludes that such an excess could be due to pions: $\sigma(dAu \rightarrow \pi^+ X) = \sigma(dAu \rightarrow \pi^- X)$, up to corrections of a few per cent related to the fact that the gold nucleus is not isoscalar. Standard sets of fragmentation functions do not predict large contributions from kaons and protons, and in the NLO calculation one ends up with $\sigma(dAu \rightarrow h^+ X)$ at most only 10% larger than $\sigma(dAu \rightarrow h^- X)$. It is hard to conceive that proton production could lead to a large enhancement of h^+ over h^- (that even increases with p_T) but, barring any experimental systematic problem, this appears to be the conclusion at present. If the final BRAHMS data continue to show this large excess, it will be a challenge to understand it in terms of a nonperturbative effect. Such an effect could, perhaps, result from coalescence of quarks from the incoming nucleon with other partons, to form a baryon. For this to work, the quarks would need to experience large transverse “kicks” and would need to lose a significant fraction of their momentum. Such a possibility could be connected to the expectations of a very strong suppression of the forward nucleon spectrum in central nucleon-nucleus collisions [28, 29].

V Conclusions and outlook

We have shown that there is an intrinsic enhancement in the ratio R_{dAu} for negatively charged hadrons, simply because of the different nature of the “projectile” (deuteron vs. proton) in the numerator and denominator of R_{dAu} . In the light of Fig. 9 the significant suppression seen by BRAHMS at $\eta = 2.2$ and $\eta = 3.2$ is even more striking than usually appreciated. The effect we have found has not been taken into account in any previous theoretical study [2, 3, 5] of the data, to our knowledge. We expect that future data for R_{dAu} for *summed* charged hadrons in this kinematic regime will show an even stronger suppression than observed for h^- , roughly by a factor 1.5. The same should happen if R_{pAu} , rather than R_{dAu} , were measured for h^- .

Because of the effect, it is entirely impossible to explain the suppression in R_{dAu} at forward rapidities by a conventional modification of the leading-twist parton densities in nuclei. However, *even if* we disregard the effect, nuclear leading-twist shadowing plays a rather unimportant role, giving at most a suppression of 15%. The reason for this is that parton momentum fractions in the gold nucleus are not very small on average even for forward kinematics, as we have shown. In other words, a large nuclear contribution originates from a range of x where nuclear

effects are known to be small (or even antishadowed). This generally sets severe limitations on the ability of *any* initial-state small- x effects to explain the observed suppression.

We have also mentioned that the fact that BRAHMS observes the cross section for $dAu \rightarrow h^+ X$ to be significantly larger than that for $dAu \rightarrow h^- X$ at $p_T > 1$ GeV, indicates the presence of sizable nonperturbative contributions possibly related to protons. It appears likely that mechanisms responsible for an enhancement of proton production then also play a role in the observed suppression of R_{dAu} . Nonperturbative production of pions, too, could play a role: coalescence effects involving spectator partons are likely to be strongly suppressed in p(d)A collisions as compared to the pp case [28]. This suppression is further enhanced when energies are large enough to resolve the small- x high gluon densities [29]. Such non-leading twist effects should decrease with increase of the transverse momentum of the pion, which is consistent with the trend in the data on R_{dAu} . On the other hand, the observed excess of $dAu \rightarrow h^+ X$ over $dAu \rightarrow h^- X$ actually *increases* with p_T , which is quite challenging to understand. Note also that the parton energy losses that would be necessary to reproduce the Brahms effect appear to be rather large: about 10% energy loss would be needed if it occurred only in the initial state before the interaction. If one assumes that the rate of energy loss is the same in the initial and final states, a loss of about 3% is necessary. For the kinematics relevant here, the suppression is more sensitive to losses in the final state since the average $\langle z \rangle$ for fragmentation was found to be substantially closer to one than the averages $\langle x_{1,2} \rangle$ in the parton densities (see Fig. 4).

To further investigate experimentally the origin of the suppression in R_{dAu} it would be useful to perform measurements of dihadron production. Within LO kinematics, the pseudorapidities of the two hadrons are related by $\eta_1 + \eta_2 = \ln(x_1/x_2)$. One may therefore single out contributions from small x_2 by demanding that both hadrons be rather forward. Fig. 10 shows this for a sample calculation. We assume that a “trigger” hadron (π^0) is detected with transverse momentum $p_{T,1} = 2.5$ and forward rapidity $2.5 \leq \eta_1 \leq 3.5$. Let the second π^0 have $1.5 \text{ GeV} \leq p_{T,2} \leq p_{T,1}$. Without any restriction on the rapidity η_2 of the second hadron, one then obtains the higher $\log_{10}(x_2)$ -distributions in Fig. 10. As expected, these look very much like the single-hadron distributions shown in Sections II and III. If now the second hadron is also in the forward region at $1.5 \leq \eta_2 \leq 4$, the lower distribution is obtained, which is entirely located at $x_2 \leq 0.01$. We also show in Fig. 10 the corresponding results for dAu collisions, using our “shadowing 1”. The shadowing effects are much more relevant for the double-forward distribution, as expected. We note that the distributions in Fig. 10 are normalized such that they sum to the cross section $d\sigma/dp_{T,1}$ in pb/GeV. It is evident that there is a significant decrease in rate for two forward hadrons. The results shown in Fig. 10 are only LO. The NLO corrections are expected to be sizable; they are available [30]. The two hadrons we have studied in Fig. 10 would be nearly

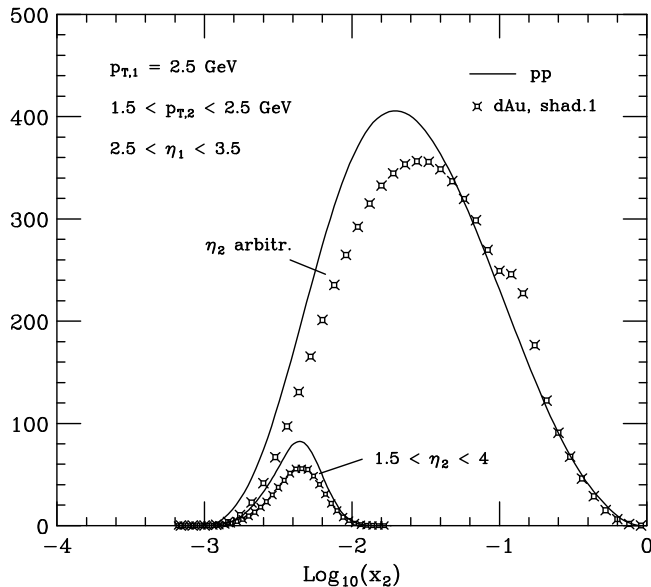


Figure 10: LO distributions in $\log_{10}(x_2)$ of the cross section $d\sigma/dp_{T,1}$ for $pp \rightarrow \pi^0\pi^0 X$ and $dAu \rightarrow \pi^0\pi^0 X$ production at $\sqrt{s} = 200$ GeV. The kinematic variables have been chosen as described in the text. Solid lines are for pp collisions and histograms are for dAu , using “shadowing 1”. The higher-lying histograms are for the case of “arbitrary” (i.e., unconstrained) η_2 , the lower ones are for $1.5 \leq \eta_2 \leq 4$.

back-to-back in azimuthal angle. Further insights into the dynamics may be gained by studying back-to-back azimuthal correlations [31, 32]. We finally note that small- x_2 effects might also become more readily accessible in conceivable future pA collisions after increase of the proton energy to 250 GeV at a later stage of RHIC operations.

Acknowledgments

We are grateful to D. de Florian, B. Jäger, and M. Stratmann for valuable help, and to L. Frankfurt, D. Kharzeev, S. Kretzer, K. Tuchin, and R. Venugopalan for useful discussions and comments. V.G. is supported by Sofia Kovalevskaya Program of the Alexander von Humboldt Foundation. M.S.’s research was supported by the DOE grant No. DE-FG02-93ER40771. W.V. is grateful to RIKEN, Brookhaven National Laboratory and the U.S. Department of Energy (contract number DE-AC02-98CH10886) for providing the facilities essential for the completion of this work.

References

- [1] I. Arsene *et al.* [BRAHMS Collaboration], arXiv:nucl-ex/0403005.
- [2] J. Jalilian-Marian, arXiv:nucl-th/0402080;
D. Kharzeev, Y. V. Kovchegov and K. Tuchin, arXiv:hep-ph/0405045;
for earlier work, see: D. Kharzeev, E. Levin and L. McLerran, Phys. Lett. B **561**, 93 (2003) [arXiv:hep-ph/0210332];
D. Kharzeev, Y. V. Kovchegov and K. Tuchin, Phys. Rev. D **68**, 094013 (2003) [arXiv:hep-ph/0307037];
J. L. Albacete, N. Armesto, A. Kovner, C. A. Salgado and U. A. Wiedemann, Phys. Rev. Lett. **92**, 082001 (2004) [arXiv:hep-ph/0307179].
- [3] J. w. Qiu and I. Vitev, arXiv:hep-ph/0405068.
- [4] D. de Florian and R. Sassot, Phys. Rev. D **69**, 074028 (2004) [arXiv:hep-ph/0311227].
- [5] R. Vogt, arXiv:hep-ph/0405060.
- [6] S. S. Adler *et al.* [PHENIX Collaboration], Phys. Rev. Lett. **91**, 241803 (2003) [arXiv:hep-ex/0304038].
- [7] J. Adams *et al.* [STAR Collaboration], Phys. Rev. Lett. **92**, 171801 (2004) [arXiv:hep-ex/0310058];
L. C. Bland [STAR Collaboration], talk at the “10th International Workshop on High-Energy Spin Physics (SPIN 03)”, Dubna, Russia, 16-20 Sep. 2003, arXiv:hep-ex/0403012.
- [8] F. Aversa, P. Chiappetta, M. Greco, and J.-Ph. Guillet, Nucl. Phys. **B327**, 105 (1989);
D. de Florian, Phys. Rev. **D67**, 054004 (2003) [arXiv:hep-ph/0210442];
B. Jäger, A. Schäfer, M. Stratmann, and W. Vogelsang, Phys. Rev. **D67**, 054005 (2003) [arXiv:hep-ph/0211007].
- [9] J. Pumplin *et al.*, JHEP **0207**, 012 (2002) [arXiv:hep-ph/0201195].
- [10] B.A. Kniehl, G. Kramer, and B. Pötter, Nucl. Phys. **B582**, 514 (2000) [arXiv:hep-ph/0010289].
- [11] M. Glück, E. Reya, and A. Vogt, Eur. Phys. J. **C5**, 461 (1998) [arXiv:hep-ph/9806404].
- [12] L. Frankfurt and M. Strikman, Eur. Phys. J. A **5**, 293 (1999) [arXiv:hep-ph/9812322].

- [13] L. Frankfurt, V. Guzey, M. McDermott and M. Strikman, JHEP **0202**, 027 (2002) [arXiv:hep-ph/0201230].
- [14] L. Frankfurt, V. Guzey and M. Strikman, arXiv:hep-ph/0303022.
- [15] K. J. Eskola, V. J. Kolhinen and P. V. Ruuskanen, Nucl. Phys. B **535**, 351 (1998) [arXiv:hep-ph/9802350];
K. J. Eskola, V. J. Kolhinen and C. A. Salgado, Eur. Phys. J. C **9**, 61 (1999) [arXiv:hep-ph/9807297];
M. Hirai, S. Kumano and M. Miyama, Phys. Rev. D **64**, 034003 (2001) [arXiv:hep-ph/0103208].
- [16] L. L. Frankfurt and M. I. Strikman, Phys. Rept. **76**, 215 (1981), *ibid.* **160**, 235 (1988).
- [17] V.N. Gribov, Sov. Phys. JETP **29**, 483 (1969) [Zh. Eksp. Tor. Fiz. **56**, 892 (1969)].
- [18] J. C. Collins, Phys. Rev. D **57**, 3051 (1998) [Erratum-*ibid.* D **61**, 019902 (2000)] [arXiv:hep-ph/9709499].
- [19] C. Adloff *et al.* [H1 Collaboration], Z. Phys. C **76**, 613 (1997) [arXiv:hep-ex/9708016].
- [20] J. Breitweg *et al.* [ZEUS Collaboration], Eur. Phys. J. C **6**, 43 (1999) [arXiv:hep-ex/9807010].
- [21] for review, see: M. Arneodo, Phys. Rept. **240**, 301 (1994).
- [22] M. Brooks [PHENIX Collaboration], talk presented at “The 17th International Conference on Ultra-Relativistic Nucleus-Nucleus Collisions (Quark Matter 2004)”, Oakland, January 2004; A. D. Frawley [PHENIX Collaboration], J. Phys. G **30**, S675 (2004) [arXiv:nucl-ex/0404009].
- [23] A. Breakstone *et al.* [ABCDHW Collaboration], Phys. Lett. B **135**, 505 (1984).
- [24] S. Kretzer, Phys. Rev. D **62**, 054001 (2000) [arXiv:hep-ph/0003177].
- [25] D. Drijard *et al.* [CDHW Collaboration], Nucl. Phys. B **208**, 1 (1982).
- [26] J. Singh *et al.* [CHLM Collaboration], Nucl. Phys. B **140**, 189 (1978).
- [27] R. Debbe [BRAHMS Collaboration], J. Phys. G **30**, S759 (2004) [arXiv:nucl-ex/0403052].
- [28] A. Berera, M. Strikman, W. S. Toothacker, W. D. Walker and J. J. Whitmore, Phys. Lett. B **403**, 1 (1997) [arXiv:hep-ph/9604299].

- [29] A. Dumitru, L. Gerland and M. Strikman, Phys. Rev. Lett. **90**, 092301 (2003) [Erratum-
ibid. **91**, 259901 (2003)] [arXiv:hep-ph/0211324].
- [30] J. F. Owens, Phys. Rev. D **65**, 034011 (2002) [arXiv:hep-ph/0110036].
- [31] J. w. Qiu and I. Vitev, Phys. Lett. B **570**, 161 (2003) [arXiv:nucl-th/0306039];
D. Kharzeev, E. Levin and L. McLerran, arXiv:hep-ph/0403271;
- [32] A. Ogawa [STAR Collaboration], talk presented at the “XIIth International Workshop on
Deep Inelastic Scattering (DIS 2004)”, Strbske Pleso, Slovakia, April 2004.